Catalysis Letters Vol. 109, Nos. 1–2, June 2006 (© 2006)
DOI: 10.1007/s10562-006-0051-9

Reactivity of aluminum spinels in the ethanol steam reforming reaction

M. Noelia Barroso, Manuel F. Gomez, Luis A. Arrúa, and M. Cristina Abello*

Instituto de Investigaciones en Tecnología Química - (UNSL-CONICET), Chacabuco y Pedernera, 5700 San Luis, Argentina

Received 1 December 2005; accepted 7 March 2006

Aluminum spinels, MAl_2O_4 with M^{2+} = Cu, Zn or Ni, were prepared by citrate method and its reactivity in the ethanol steam reforming reaction was studied at 500 °C. They were characterized by TG, BET surface area, XRD, FTIR and TPR techniques. The catalytic behavior depended strongly on the nature of divalent metal which determines the physico-chemical properties of samples. In all cases, very active catalysts with a complete ethanol conversion were reached. Hydrogen yield follows the order of ZnAl > NiAl > CuAl.

KEY WORDS: ethanol; steam reforming; hydrogen production; spinel catalysts.

1. Introduction

Hydrogen is considered the future fuel and it will become the major energy source as the fossil resources become insufficient to satisfy the global energy demand. Different hydrogen production methods can be used: water electrolysis, gasification, partial oxidation reactions of heavy oil and steam reforming reactions. Until now the hydrocarbon steam reforming, specially of methane, is the most widespread and economic way to produce hydrogen [1].

An attractive alternative to hydrogen production is the ethanol steam reforming [2–15]. Ethanol has several advantages compared to other raw materials but the most important is its renewable origin and the consequent reduction in CO_2 emission. It has a relatively high hydrogen content and its reaction in the presence of water is able to produce six moles of hydrogen per mol of fed ethanol.

$$C_2H_5OH + 3H_2O \rightarrow 2CO_2 + 6H_2. \qquad (1)$$

From a thermodynamic point of view, the reaction (1) is highly favored, $\Delta G^{o}_{500\,^{\circ}C} = -125.7$ kJ mol^{-1}, but several reactions are involved and in general, the reactor effluent contains a wide range of liquid and gaseous products. The best catalyst for the reaction (1) requires a surface capable of breaking the ethanol C–C bond and of oxidizing both carbon atoms to CO_2. Besides, it should be unable to promote the oxidation of H_2 and other C–C bond formation reactions.

In previous works, we studied the ethanol steam reforming reaction over MZnAl ternary oxides (M = Ni or Cu ranging from 1 to 25 wt%) [16,17]. These systems were very active with 100% of ethanol conversion at 500–600 °C and the product distribution depended on composition of catalysts. The formation of a highly crystalline spinel phase of $ZnAl_2O_4$ was observed on NiZnAl catalysts calcined at 700 °C. From characterization results there were some evidences of $NiAl_2O_4$ formation. Similar results were obtained on CuZnAl system where the $CuAl_2O_4$ formation could not be ruled out. Recently, it has been also observed a higher use of spinels as catalyst or supports in reforming reactions [18–20]. Valenzuela et al. [21] have studied $ZnAl_2O_4$ as a support of Pt and Pt–Sn catalysts and they have reported a increase in the thermal stability compared to the conventional support such as γ-Al_2O_3. With the aim of having information about the reactivity of pure phases, this work presents the preparation, characterization and catalytic activity over spinel-type MAl_2O_4 with M^{2+} = Cu, Zn or Ni.

2. Experimental

2.1. Catalyst preparation

MAl_2O_4 spinels (M = Zn, Cu, Ni) were prepared by the citric method. Citric acid was added to an aqueous solution that contained all the required ions as metal nitrates ($Cu(NO_3)_2{\cdot}3H_2O$; $Ni(NO_3)_2{\cdot}6H_2O$; $Zn(NO_3)_2{\cdot}6H_2O$; $Al(NO_3)_3{\cdot}9H_2O$). An equivalent of acid per total equivalent of metals was used. The solution was stirred for 10 min and held at boiling temperature for 30 min. Then, it was evaporated in a revolving flask under a pressure of a few mm Hg at 75 °C until a viscous liquid was obtained. Finally, dehydration was completed by drying the sample in a vacuum oven at 100 °C for 16 h. Samples were calcined in a step process, first in N_2 flow for 2 h and then, in O_2 (10%)/N_2 flow at 500 °C for 5 h. Finally,

---

*To whom correspondence should be addressed.
E-mail: cabello@unsl.edu.ar

the temperature was raised at 700 °C and kept for 2 h. They were denoted as MAl.

2.2. Catalyst characterization

All samples were characterized using different physico-chemical methods.

B.E.T Surface area. BET surface areas were measured by using a Micromeritics Accusorb 2100E instrument by adsorption of nitrogen at −196 °C on 200 mg of sample previously degassed at 200 °C for 2 h under high vacuum atmosphere.

X-ray Diffraction (XRD). XR diffraction patterns were obtained with a RIGAKU diffractometer operated at 30 kV and 20 mA by using Ni-filtered Cu K_α radiation ($\lambda = 0.15418$ nm) at a rate of de 3° min^{-1} from $2\theta = 20°$ to 80°. The powdered samples were analyzed without previous treatment after deposition on a quartz sample holder. The identification of crystalline phases was made by matching with the JCPDS files. XRD patterns corresponding to reduced samples were obtained after TPR experiments.

Infrared spectroscopy (IR). IR spectra were recorded by a Nicolet Protégé 460 Infrared spectrometer, in the region 4000–200 cm^{-1} with a resolution of 4 cm^{-1}. Compressed KBr pellets containing 1 wt% of a sample were employed. Each spectrum was collected by co-adding of minimum 32 scans.

Thermal gravimetry (TG). The analyses were recorded by using TGA 51 Shimadzu equipment. The samples, c.a. 15 mg, have been placed in a Pt cell and heated from room temperature to 1000 °C at a heating rate of 10 °C min^{-1} with a N_2 flow of 50 ml min^{-1}.

Temperature programmed reduction (TPR). Studies were performed in a conventional TPR equipment. This apparatus consists of a gas handling system with mass flow controllers (Matheson), a tubular reactor, a linear temperature programmer (Omega, model CN 2010), a PC for data retrieval, a furnace and various cold traps. Before each run, the samples were oxidized in a 50 ml min^{-1} flow of 20 vol% O_2 in He at 300 °C for 30 min. After that, helium was admitted to remove oxygen and then the system cooled at 25 °C. The samples were subsequently contacted with a 50 ml min^{-1} flow of 5 vol% H_2 in N_2 and heated, at a rate of 5 °C min^{-1}, from 25 °C to a final temperature of 700 °C and held at 700 °C for 1 h. Hydrogen consumption was monitored by a thermal conductivity detector after removing the water formed. The characteristic number P proposed by Malet and Caballero [22] defined as $\beta S_o/V^*C_o$, where S_o is the initial amount of reducible species in the sample (μmol), V* is the total flow rate (ml min^{-1}), C_o the initial hydrogen concentration in the feed (μmol ml^{-1}) and β the heating rate (°C min^{-1}) was ≈10 °C in order to obtain an unperturbed reduction profile.

2.3. Catalytic test

The ethanol steam reforming reaction was carried out in a fixed-bed quartz tubular reactor operated at atmospheric pressure. The reactor is encased in a furnace, which is controlled by a programmable temperature controller. The reaction temperature was measured with a coaxial thermocouple. The feed was a gas mixture of ethanol, water and helium (free of oxygen). Ethanol and water were fed through of independent saturators before mixing. The flow rates of gas stream were controlled by mass flowmeters. The flow rate was 70 ml min^{-1} at room temperature with an ethanol molar composition of 3%. The H_2O:C_2H_5OH molar ratio = 3.8 in all experiments. The catalyst weight was 0.3 g (0.3–0.4 mm particle size range selected after preliminary mass transport experiments to minimize diffusional resistances). In all experiments the W/F′ was 1.8 h where W and F′ are catalyst weight (g) and flow rate of ethanol (g h^{-1}). The catalyst was heated to the reaction temperature under He flow, then the mixture with $C_2H_5OH + H_2O$ was allowed to enter into the reactor to carried out the catalytic test. The reactants and reaction products were analyzed on-line by gas chromatography. H_2, CH_4, CO_2 and H_2O were separated by a 1.8 m Carbosphere (80–100 mesh) column and analyzed by TC detector. Besides, CO was analyzed by a flame ionization detector after passage through a methanizer. Higher hydrocarbons and oxygenated products (C_2H_4O, C_2H_4, C_3H_6O, C_2H_5OH, etc) were separated in Rt-UPLOT capillary column and analyzed with FID using N_2 as carrier gas. The activity was measured at 500 °C for 5 h and the yield in C-products was defined as

$$\text{Yi} = \frac{F_i^{out}}{\nu F_{EtOH}^{in}}$$

being F: molar flow; ν: stoichiometry factor; i = C-product. For hydrogen the yield, Y_{H2}, was expressed as mol H_2/mol C_2H_5OH fed

The homogeneous contribution was tested with the empty reactor. These runs showed no activity at 500°C whereas the ethanol conversion was 3% at 600 °C being acetaldehyde the only product.

3. Results and discussion

Aluminum spinels are prepared by the citrate method [23], which is known to be a powerful method for making homogeneous oxides containing two or several metallic elements. In all cases, precursors uniformly colored and completely amorphous to X-ray diffraction are obtained. The dried sample decompositions are studied by thermogravimetry under a N_2 flow to avoid the fast and exothermal decomposition of precursors. For Zn and Ni aluminates the most important weight loss is between 370 and 500 °C with a maximum around

420 and 414 °C, respectively. The total weight loss amounts to 73.1 and 72% of the original weight which is very near to those calculated for the thermal decomposition of precursors into $ZnAl_2O_4$ and $NiAl_2O_4$, respectively. No significant weight loss is detected after 500 °C that can be attributed to the formation of a pure oxide system. Taking into account these results, the first step of calcination procedure for these samples is carried out at 450 °C under nitrogen flow. For the sample containing Cu the most important weight loss is at 300 °C due to the catalytic activity of copper for burning citrate chains. In this case, the first calcination step is running at 300 °C. The second calcination step to eliminate the residual carbon as is described in the experimental part is identical for all samples. These results and other characteristics of spinel-type samples are shown in Table 1.

XRD analyses are carried out to examine the catalyst structure after calcination, denoted as fresh sample, hydrogen reduction and used in ethanol steam reforming. The X-ray patterns for ZnAl spinel are shown in figure 1. On fresh sample, figure 1a, the diffraction lines of the $ZnAl_2O_4$ spinel phase (2θ = 36.9°, 31.3°, 59.4° and 65.3°, JCPDS-5-669) are intense and symmetric indicating a high crystallinity. The intensity ratio I_{311}/I_{220} being I_{311} and I_{220} reflection line intensities of basal planes 311 and 220 is strongly indicating that the $ZnAl_2O_4$ is a normal spinel [24]. For reduced and used samples, figure 1(b) and (c), the peaks are not practically altered which is an indication of a high structural stability.

For NiAl catalyst, figure 2, the reflection lines due to the formation of $NiAl_2O_4$ (2θ = 37°, 45°, 31.4°, 59.6° and 65.5°, JCPDS-78-0552) are observed in the fresh sample. They are broad showing that the crystallite size is small. The presence of NiO (2θ = 43.3°, 37.3°, 62.9°, JCPDS-4-835) is also detected. Al_2O_3 cannot be ruled out. Al_2O_3 usually shows poor crystallinity and its amount should be small due to its consumption in the spinel formation. Besides, the γ-Al_2O_3 is a spinel type phase and their diffraction peaks closely coincide. In reduced and used samples the XDR patterns show the peaks corresponding to Ni^0 (2θ = 44.5°, 51.8°, 76.4°, JCPDS-4-850), figure 2(b, c). The reflection lines of $NiAl_2O_4$ are also observed indicating that a partial reduction occurs as under H_2 atmosphere as in reforming conditions. The reduction extent is higher under hydrogen reduction (up to 700 °C) than under reforming conditions (at 500 °C).

For CuAl catalyst, figure 3, the reflection lines corresponding to CuO (2θ = 35.5°, 38.9°, JCPDS-41-0254) and $CuAl_2O_4$ (2θ = 36.7°, 31.3°, 65.3°, 59.4°, 44.8°, 55.7°, 77.5°, JCPDS33-0448) become evident in the fresh sample. The calcination temperature is not enough to lead to the formation of pure copper aluminate. The presence of Al_2O_3 could not be ruled out either. This tendency of phase separation has just been observed in

Table 1
Characteristics of MAl_2O_4 samples prepared by citric method

Sample	M wt%	M/Al	T_{TG}, °C	S_{BET}, $m^2\ g^{-1}$
ZnAl	34.7	0.49	420 (73.1%)	58
NiAl	33.2	0.5	414 (72.0%)	133
CuAl	32.7	0.48	300 (73.4%)	53

M = Zn, Ni or Cu. Values between brackets represent the weight loss in TG experiments.

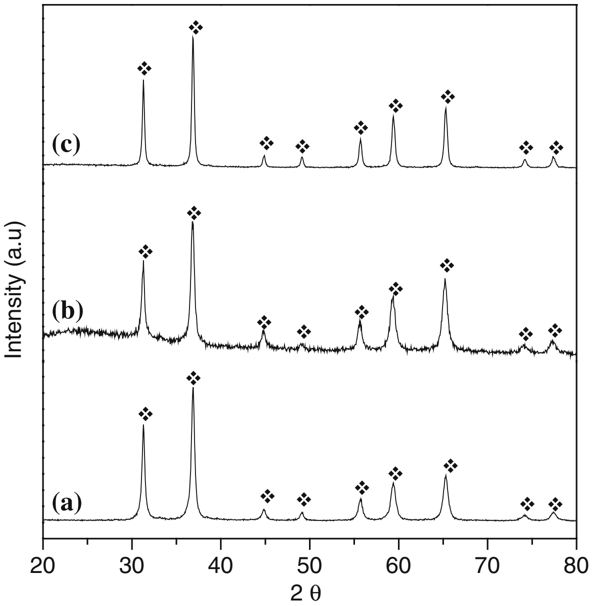

Figure 1. XRD patterns of ZnAl sample. (a) fresh, (b) reduced under H_2 at 700 °C, (c) used in reaction.: $ZnAl_2O_4$.

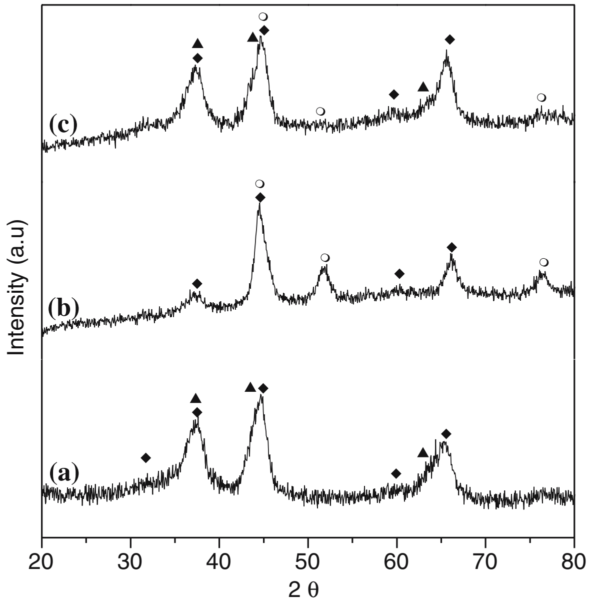

Figure 2. XRD patterns of NiAl sample. (a) fresh, (b) reduced under H_2 at 700 °C, (c) used in reaction. ♦: $NiAl_2O_4$; ▲: NiO; ○ Ni.

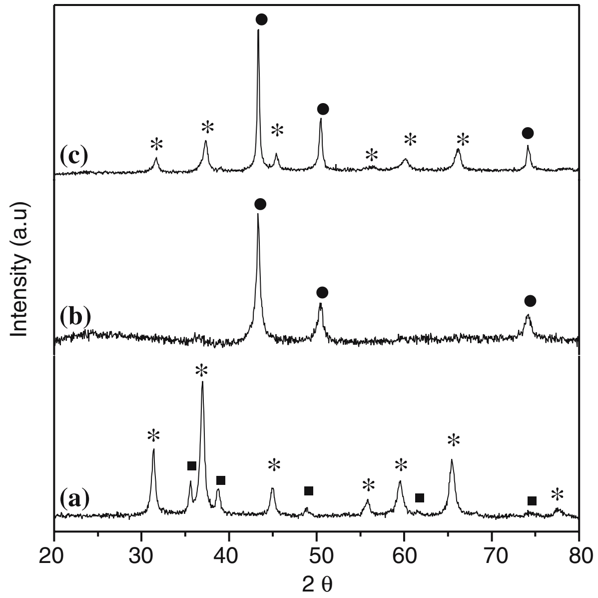

Figure 3. XRD patterns of CuAl sample. (a) fresh, (b) reduced under H_2 at 700°C, (c) used in reaction. *: $CuAl_2O_4$; ■: CuO; ●: Cu.

literature [25]. In the reduced sample, figure 3b, the results show very sharp peaks of metallic copper (2θ = 43.3°, 50.4°, 74.1°, JCPDS 4-0836). However, after being used in reaction the intensities of reflection lines corresponding to spinel phase decrease indicating that the reduction is not complete under reforming conditions in spite of the high reaction temperature, figure 3c.

Figure 4 reports the IR spectra of samples. The spectrum of ZnAl reveals the characteristic structure of a normal spinel. Three peaks centered at 660, 550 and 495 cm^{-1} due to the stretching mode of Al–O in octahedral coordination state (AlO6 octahedral units) [26] are observed in agreement with XRD results. Residual organic and hydroxyl groups are absent. IR spectra of CuAl and NiAl samples are dominated by a strong and broad absorption band in the region of 900–400 cm^{-1} related to the inorganic network corresponding to Al–O stretching frequencies (AlO6 and AlO4). These spectra are suggesting the presence of Al in tetrahedral coordination. In literature, it has been reported that the parameter η of $NiAl_2O_4$ (defined as the fraction of divalent metal ions in octahedral coordination) is 0.76 which is indicating that Ni has a tendancy to form spinel with some inversion extent [27]. Similar results are obtained for CuAl sample, figure 4c. It is known that Cu^{2+} ions show the Jahn–Teller effect that favors the formation of distorted octahedral structures [28].

The spectrum of NiAl sample shows bands at 3500–3000 cm^{-1} ascribed to surface adsorbed water and chemically bonded hydroxyl groups that have not completely disappeared after calcination. Besides, bands between 1600–1400 cm^{-1} are observed. IR spectra of the sample calcined at 700 °C at different times show that the intensities of these bands markedly decrease with calcination time. Then, they could correspond to the asymmetric and symmetric vibrations of COO^- groups [29] remaining of preparation. However, these bands are still weakly visible after a treatment at 1000 °C. This fact could be an indication that bicarbonate species are also formed on Al_2O_3 owing to the readsorption of CO_2 upon exposing the sample to the atmosphere.

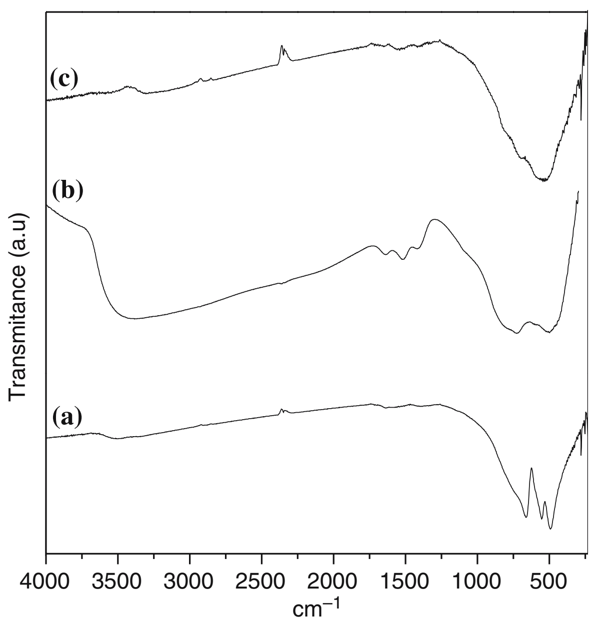

Figure 4. FTIR spectra of (a) ZnAl, (b) NiAl, and (c) CuAl samples recorded in air at room temperature using the KBr method.

The reducibility of samples is examined by temperature programmed reduction, figure 5. A almost flat TPR profile is obtained for ZnAl in agreement with

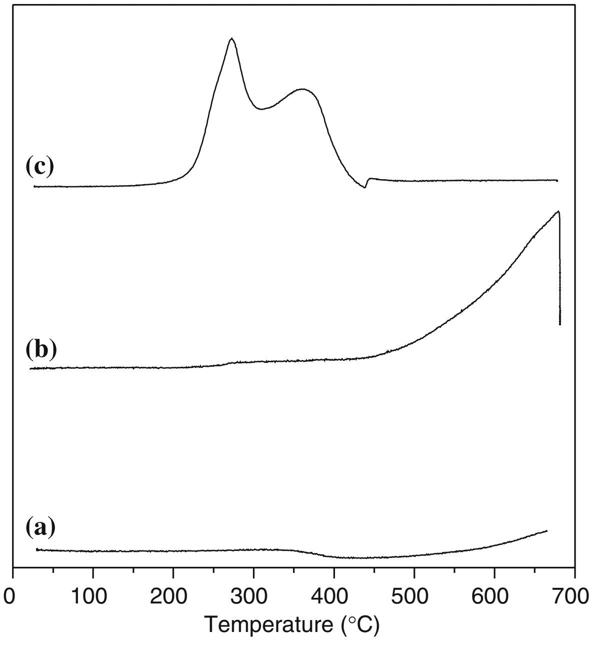

Figure 5. TPR profiles of (a) ZnAl, (b) NiAl, and (c) CuAl samples.

XRD. On reduced sample, figure 1b, the peaks assigned to $ZnAl_2O_4$ are not practically altered. For NiAl the H_2 consumption in TPR becomes significant around 600 °C due to the reduction of Ni^{2+} to Ni^0. Under the experimental TPR conditions used in this work nickel species could not be reduced completely. For CuAl, TPR profile presents two hydrogen consumption bands, the first peak at 274 °C and the second one at 360 °C can be attributed to the reduction of different Cu^{2+} species associated with CuO and $CuAl_2O_4$, respectively. This peak assignation was confirmed by means of a TPR experiment performed under the same conditions. In this case the experiment was stopped after the appearance of the first reduction peak. Then, the sample was purged and quickly cooled down with helium. The XRD pattern of this sample only revealed the presence of Cu^0 and $CuAl_2O_4$. Then, the reduction of Cu^{2+} from CuO occurs at lower temperature than that of $CuAl_2O_4$, which is in agreement with literature [30].

The total H_2 consumption indicates that all Cu^{2+} species are reduced to Cu^0 at temperatures below the reaction temperature. However, CuAl sample shows a quite easy reducibility, a partial reduction is observed under reforming conditions, figure 3c.

3.1. Catalytic steam reforming results

The activity of aluminum spinels is tested in the steam reforming of ethanol. A very high ethanol conversion is observed on all catalysts with important differences in the product distribution. The main carbon compounds obtained at 500 °C are C_3H_6O, C_2H_4O, C_2H_4, C_3H_6, CH_4, CO, and CO_2 depending on divalent cation. The product distribution indicates that the steam reforming reaction is negligible over the three samples and other ethanol reactions takes place; mainly ethanol dehydrogenation (Eq. (2)) to acetaldehyde, ethanol dehydration to ethylene (Eq. (3)), acetaldehyde decomposition to acetone (Eq. (4))

$$C_2H_5OH \rightarrow C_2H_4O + H_2 \tag{2}$$

$$C_2H_5OH \rightarrow C_2H_4 + H_2O \tag{3}$$

$$2C_2H_4O + H_2O \rightarrow C_3H_6O + CO_2 + 2H_2. \tag{4}$$

The catalytic behavior of ZnAl spinel with reaction time is shown in figure 6. It is observed that ZnAl produces an important fraction of undesirable compounds being acetone the main product. The high acetone yield (57.3% after 1 h in reaction) is an indication that $ZnAl_2O_4$ mainly promotes the chain grown. The H_2 yield is 2.35 mol H_2/mol C_2H_5OH at the same reaction time. The ethanol conversion begins to decrease (98%) after 5 h in reaction. It can be seen that acetaldehyde slowly increases with time at the expense of acetone, CO_2 and H_2 which indicates that the decomposition of ethanol to acetone via acetaldehyde, Eq. (4), is depressed. This sample exhibits the best performance in hydrogen formation. Besides, its high thermal resistance under reforming conditions becomes an attractive support for ethanol reforming catalysts.

Over CuAl sample the dehydration of ethanol to ethylene, Eq. (3), is the most important reaction with a yield to C_2H_4 of 76.7% at 60 min on stream. The ethanol conversion decreases from 100 to 95% after 280 min in time on stream with some differences in the product distribution, figure 7. In particular, the decrease in conversion is accompanied by a decrease in C_2H_4 formation. It is known that ethylene is a precursor of coke, which can deactivate the catalyst. The acetaldehyde formation

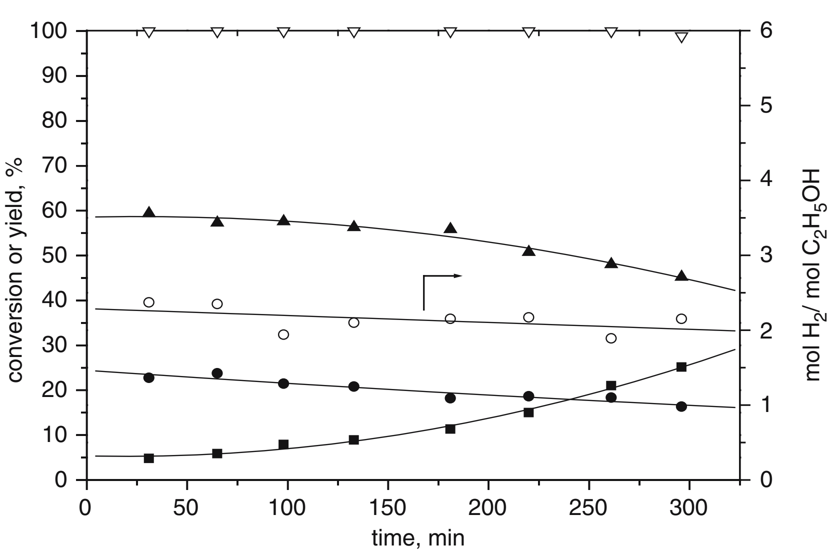

Figure 6. Catalytic performance of ZnAl sample at 500°C and atmospheric pressure. ▽: C_2H_5OH conversion; ○: mol H_2/mol C_2H_5OH; ■: CH_3CHO; ▲: $(CH_3)_2CO$, ●: CO_2.

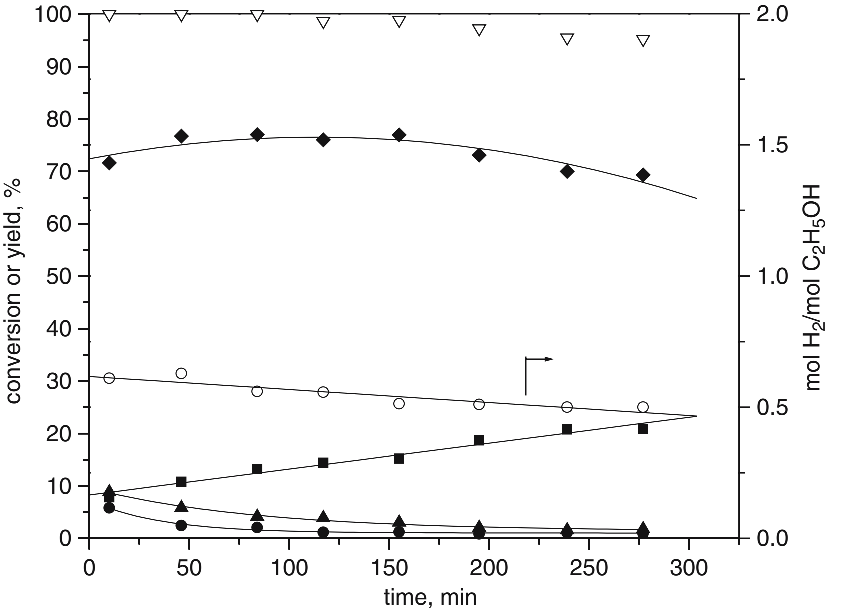

Figure 7. Catalytic performance of CuAl sample at 500°C and atmospheric pressure. ▽: C_2H_5OH conversion; ○: mol H_2/mol C_2H_5OH; ■: CH_3CHO; ♦: C_2H_4, ▲: $(CH_3)_2CO$, ●: CO_2.

increases with time being 21% at c.a. 300 min. The H_2 yield is the lower one observed, around 0.5 mol H_2/mol C_2H_5OH.

The catalytic behavior on NiAl sample is intermediate with a H_2 yield of 1.67 mol H_2/mol C_2H_5OH which is nearly constant during 5 h in reaction. Over this sample ethanol dehydration and decomposition to acetone take place to a large extent. The decomposition of ethanol to acetone via acetaldehyde decreases gradually while the dehydration increases. Acetone yield decreases from 31 to 6.6% whereas ethylene yield increases from 35 to 58% after 5 h, figure 8. The increase in ethylene throughout the test indicates a progressive modification of the catalyst. In fact, coke is observed on the spent catalyst.

In order to understand the catalytic behavior and the influence of coke formation, temperature programmed oxidation experiments of the spent samples were carried out with the TG technique. From an analysis of results shown in figure 9 and a visual observation of samples it can be concluded that coke is mainly deposited on CuAl and NiAl. For ZnAl

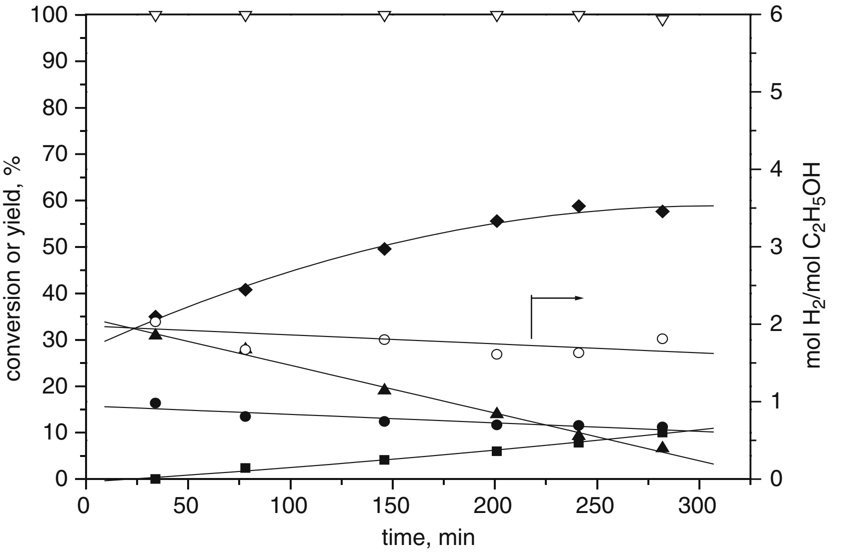

Figure 8. Catalytic performance of NiAl sample at 500°C and atmospheric pressure. ▽: C_2H_5OH conversion; ○: mol H_2/mol C_2H_5OH; ■: CH_3CHO; ♦: C_2H_4, ▲: $(CH_3)_2CO$, ●: CO_2.

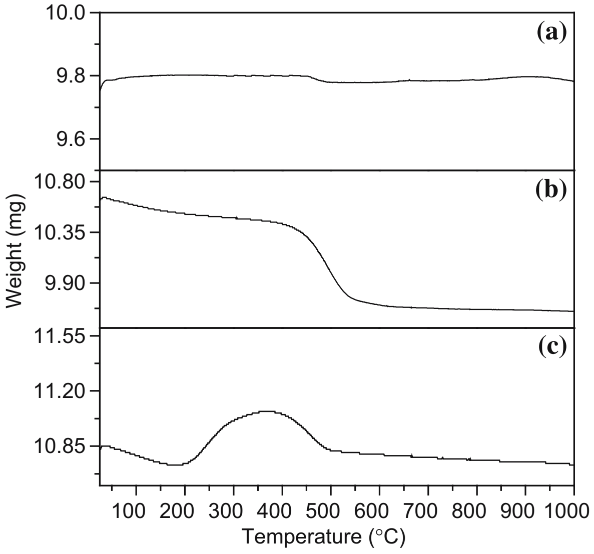

Figure 9. TG behavior of spent samples under air after 4 h on stream (a) ZnAl, (b) NiAl, and (c) CuAl.

sample a small weight loss between 450 and 500 °C is detected, curve (a). For NiAl sample, curve (b), two zones of weight loss are observed. An initial weight loss up to 400 °C due to dehydratation and removal of easily oxidizable carbonaceous species and an abrupt weight loss between 400 and 600 °C attributed to coke combustion in agreement with literature data [19]. The coke could be deposited on metallic species and aluminate matrix. For CuAl sample a different behavior is observed, curve (c). The initial weight loss is ascribed to thermal desorption of H_2O; the gain weight between 200 and 360 °C is due to oxidation of Cu to CuO; and finally the weight loss from 360 to 500 °C is attributed to burning off the coke. This could be an evidence that carbon is mainly deposited on aluminate matrix. In both samples, this carbon accumulation process should be responsible of changes in the product distribution.

4. Conclusions

Aluminum spinels were very active in the catalytic conversion of ethanol at 500 °C. In all cases, a complete initial alcohol conversion was obtained. However, the product distribution depends strongly on the nature of divalent metal which determines the physico-chemical properties of samples. Hydrogen yield follows the order of ZnAl > NiAl > CuAl. Although the best performance in hydrogen production is $ZnAl_2O_4$, this spinel phase seems to be a good support due to its high thermal resistance under reforming conditions.

Acknowledgments

Financial supports are acknowledged to CONICET, ANPCyT and Universidad Nacional de San Luis.

References

[1] J.N. Armor, Appl. Catal. A: Gen. 176 (1999) 159.
[2] C. Diagne, H. Idriss and A. Kiennemann, Catal. Comm. 3 (2002) 565.
[3] S. Cavallaro, V. Chiodo, S. Freni, N. Mondello and F. Frusteri, Appl. Catal. A: Gen. 249 (2003) 119.
[4] D. Liguras, D. Kondarides and X. Verykios, Appl. Catal. B: Environ. 43 (2003) 345.
[5] F. Frusteri, S. Freni, L. Spadaro, V. Chiodo, G. Bonura, S. Donato and S. Cavallaro, Catal Comm. 5 (2004) 611.
[6] V. Klouz, V. Fierro, P. Denton, H. Katz, J. Lisse, S. Bouvot-Mauduit and C. Mirodatos, J. Power Sources 105 (2002) 26.
[7] A. Kaddouri and C. Mazzocchia, Catal. Comm. 5 (2004) 339.
[8] F. Mariño, M. Boveri, G. Baronetti and M. Laborde, Int. J. Hydrogen Energy 29 (2004) 67.
[9] S. Freni, S. Cavallaro, N. Mondello, L. Spadaro and F. Frusteri, Catal Comm. 4 (2003) 259.
[10] J. Llorca, N. Homs, J. Sales, J.L.G. Fierro and P. Ramirezdela Piscina, J. Catal. 222 (2004) 470.
[11] J. Sun, X. Qiu, F. Wu, W. Zhu, W. Wang and S. Hao, Int. J. Hydrogen Energy 29 (2004) 1075.
[12] F. Auprête, C. Descorme and D. Duprez, Catal. Comm. 3 (2002) 263.
[13] F. Mariño, G. Baronetti, M. Jobbagy and M. Laborde, Appl. Catal. A: Gen. 238 (2003) 41.
[14] F. Frusteri, S. Freni, V. Chiodo, L. Spadaro, O. Di Blasi, G. Bonura and S. Cavallaro, Appl. Catal. A: Gen. 270 (2004) 1.
[15] A.J. Akande, R.O. Idem and A.K. Dalai, Appl. Catal. A: Gen. 287 (2005) 159.
[16] M.N. Barroso, M.F. Gomez, L.A. Arrua and M.C. Abello, Chem. Eng. Trans. 4 (2004) 265.
[17] Barroso M.N., Gomez M.F., Arrua L.A., Abello M.C. *Appl. Catal. A. Gen*, (in press).
[18] F. Auprete, C. Descorme, D. Duprez, D. Casanave and D. Uzio, J. Catal. 233 (2005) 464.
[19] J. Guo, H. Lou, H. Zhao, D. Chai and X. Zheng, Appl. Catal. A: Gen. 273 (2004) 75.
[20] T. Yohei, K. Ryuji, T. Tatsuya and E. Koichi, Appl. Catal. B. Environ. 57 (2005) 211.
[21] M.A. Valenzuela, J-P Jacobs, P. Bosch, S. Reijne, B. Zapata and H.H. Brongersma, Appl. Catal. A: Gen. 148 (1997) 315.
[22] P. Malet and A. Caballero, J. Chem. Soc. Faraday Trans. 84 (1988) 2369.
[23] Ph. Courty, H. Ajot and Ch. Marcilly, Powder Technol. 7 (1973) 21.
[24] Barroso M.N., Gomez M.F., Andrade Gamboa J., Arrua L.A., Abello M.C. *J. Phys. Chem. Solids* (in press).
[25] F. Meyer, R. Hepelmann, S. Mathur and M. Veith, J. Mater. Chem. 9 (1999) 1755.
[26] S. Mathur, M. Veith, M. Haas, H. Shen, N. Lecerf and V. Huch, J. Am. Ceram. Soc. 84 (2001) 1921.
[27] A. Bielanzki and J. Haber, *Oxygen in Catalysis* (Marcel Dekker, New York, 1991) 29Cap. I.
[28] M. Turco, G. Bagnasco, U. Costantino, F. Marmottini, T. Montanari, G. Ramis and G. Busca, J. Catal. 228 (2004) 43.
[29] J.I. Di Cosimo and C.R. Apesteguía, J. Catal. 116 (1989) 71.
[30] S. Gusi, F. Trifiro and A. Vaccari, Reactivity of solids 2 (1986) 59.